



White Paper on GENQEC Model in Power System Studies

WECC PPMVDWG

August 12, 2021

Introduction.....3

The GENQEC model.....3

 GENQEC model structure3

GENQEC model application to different types of generators.....5

 GENQEC model parameters5

 Round-rotor generator (Model 2.2 in IEEE Std 1110, second-order standard model)5

 Salient-pole generator (Model 2.1 in IEEE Std 1110, second-order standard model).....5

Determine *K_w*6

 Step 1. Gather parameters and field measurements for calculation7

 Step 2. Determine field current base value.....8

 Step 3. Linear regression on ***L_d*** to determine ***K_w***9

 Step 4. (Optional) VEE Curve Results Comparison with Determined ***L_d*** and ***K_w***11

Existing generator model migration to GENQEC12

 Round-rotor generator (GENROU, GENROE to GENQEC)12

 Salient-pole generator (GENSAL, GENSAE to GENQEC).....12

Appendix A.....13

 GENQEC model block diagram and its equivalent circuit representation.....13



Introduction

The WECC Modeling and Validation Subcommittee (MVS) approved the GENQEC synchronous generator model on December 3, 2020, after the implementation and benchmark among the commonly used power system analysis software (PSLFTM, PSS[®]E, PowerWorld Simulator and DSAToolsTM/TSAT [1]). The GENQEC keeps the parameter compatibility with the earlier second-order generator dynamic models such as GENROU, GENSAL, with major improvements in saturation treatment. Compared with currently used generator model GENTPJ in North America, GENQEC model has proven dynamic performance improvement through theoretical analysis and simulation results. The steady-state accuracy improvement on modeled field current has been proven using field test data from over one hundred generators with capacity ranging from 4 MVA to 835 MVA.

This white paper is intended to serve as a technical reference for those interested to validate synchronous generator model parameters using GENQEC model. The method is based on the improvement to generator decrement test in [2].

The GENQEC model

GENQEC model structure

GENQEC model was developed from the second-order generator equivalent circuits given in the IEEE Standard 1110. The full derivation process of the block diagram is given in [3] [4] and provided in Appendix A of this White Paper. The most distinctive difference of the GENQEC model from all previous generator models is that it uses a completely new method to include saturation effect in positive sequence generator model to achieve good accuracy. The root of the GENQEC model could be traced to the zero-power-factor characteristics, on which the Potier Reactance is derived. A machine dependent compensation factor, K_w , is introduced in GENQEC model. The meaning of K_w is illustrated in Figure 1 below, and more detail of this compensation factor is explained in [5].

Table 1 compares the major difference between GENQEC and several commonly available second-order models [6]. The improvement of GENQEC over the previous models can be seen from various aspects of the new implementation method of magnetic saturation and generator field current compensation.

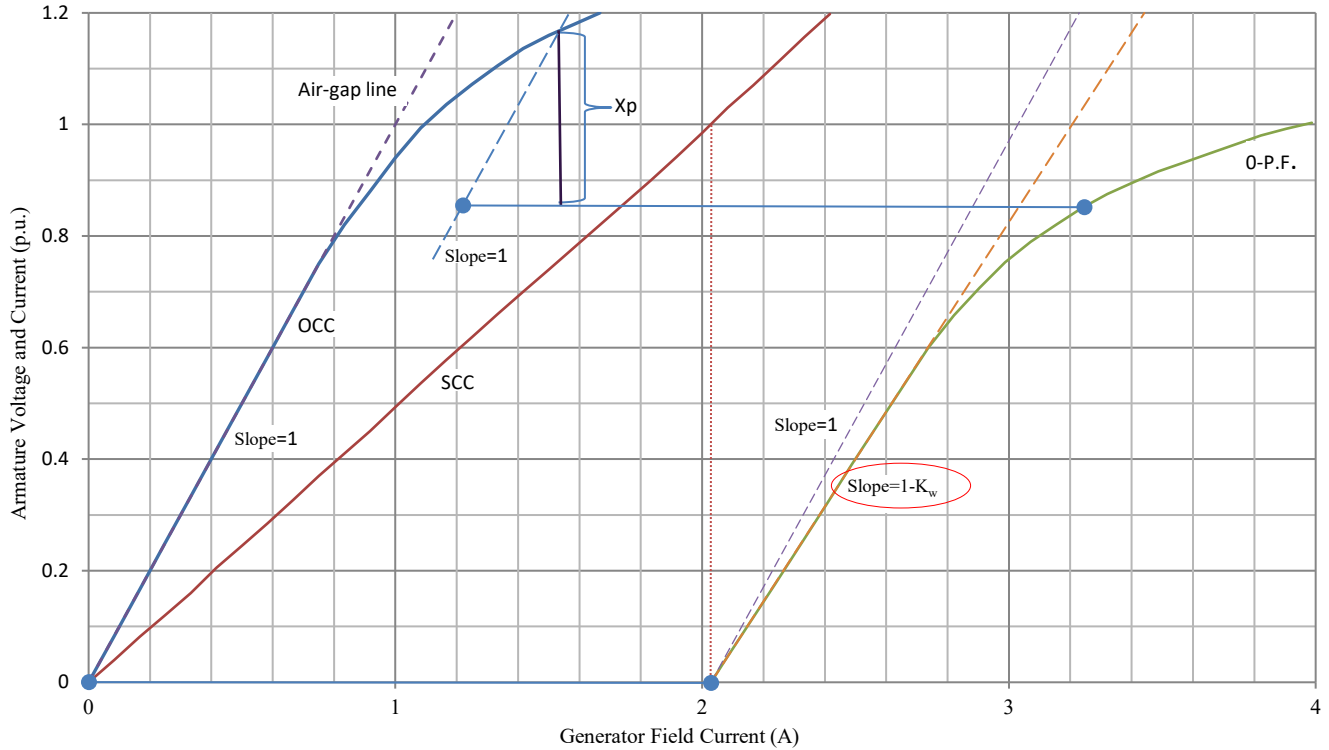


Fig. 1 Generator Saturation Characteristics, Potier Reactance and Kw in GENQEC Model

Table 1. Characteristic Comparison of second-order Generator Dynamic Models

| | Characteristic of Model | GENQEC | GENTPJ | GENROU | GENSAL |
|----|---|--------|-----------|-----------|----------------------|
| #1 | Magnetic saturation impacts all inductances | YES | YES | NO | NO |
| #2 | Magnetic saturation impacts Time Constants | YES | NO | NO | YES |
| #3 | +Id (+Mvar) cause additional increase of If | YES | YES | NO | NO |
| #4 | -Id (-Mvar) cause extra decreases of If | YES | NO | NO | NO |
| #5 | D-axis and Q-axis degree of magnetic saturation | Same | Different | Different | No Q-axis saturation |

GENQEC model application to different types of generators

GENQEC model parameters

GENQEC model uses classical representation of the standard generator parameters. Refer to Appendix A for parameter derivation from its X_{ad} -base reciprocal equivalent circuit representations.

| Description |
|--|
| Sat_{Flag} , Saturation function selection flag (0-Exponential; 1-Scaled quadratic; 2-Quadratic) |
| T'_{do} (sec), d-axis transient rotor time constant |
| T''_{do} (sec), d-axis sub-transient rotor time constant |
| T'_{qo} (sec), q-axis transient rotor time constant |
| T''_{qo} (sec), q-axis sub-transient rotor time constant |
| H (>0), Inertia constant |
| D (pu), Damping factor |
| X_d , d-axis synchronous reactance |
| X_q , q-axis synchronous reactance |
| X'_d , d-axis transient reactance |
| X'_q , q-axis transient reactance |
| X''_d , d-axis sub-transient reactance |
| X''_q , q-axis sub-transient reactance |
| X_l , stator leakage reactance |
| S(1.0), saturation factor at 1.0 pu flux |
| S(1.2), saturation factor at 1.2 pu flux |
| K_w ($0 < K_w < 0.4$), rotor field current compensation factor |

Round-rotor generator (Model 2.2 in IEEE Std 1110, second-order standard model)

Rotor d-axis: Rotor field winding and one equivalent damper winding

Rotor q-axis: Two equivalent damper windings

- Use “standard” generator model parameters including all synchronous, transient and sub-transient model parameters on d-axis and q-axis.

Salient-pole generator (Model 2.1 in IEEE Std 1110, second-order standard model)

Rotor d-axis: Rotor field winding and one equivalent damper winding

Rotor q-axis: One equivalent damper winding only

- Set $L_q = L'_q$; and T'_{qo} to an extremely big number such as 999. The rest of the parameters are “standard” generator model parameters.



Determine K_w

Since GENQEC model was developed from the second-order generator equivalent circuits given in the IEEE Standard 1110. All parameters are standard generator parameters which can be achieved by using the testing method given in IEEE Standard 115. Only K_w in GENQEC needs special attention. This chapter introduced a simple and practical method to obtain the compensation factor K_w for GENQEC model.

K_w was defined as the slope difference between the linear regions of the zero-power-factor line (0-P.F.) and the open circuit characteristics (OCC), as seen in Fig. 1. The consideration of applying the K_w factor can be found in [5], and the GENQEC equivalent circuits are given in Appendix A. This session will focus on determining the K_w factor in practice, from field measurement data through calculation.

From GENQEC model block diagram, in steady state when $\omega = 1$, the K_w factor can be obtained from the below relation when a constant, unsaturated generator synchronous inductance L_d is known.

$$L_d i_d = (1 - K_w i_d) I_{fd} - (1 + S_a)(V_q + R_a i_q) - S_a L_l i_d \quad (1)$$

Where,

L_d : Generator d-axis synchronous inductance (also will be determined from this method)

i_d : D-axis component of generator stator current (calculated from measurements, P, Q, Vt, etc.)

i_q : Q-axis component of generator stator current (calculated from measurements, P, Q, Vt, etc.)

I_{fd} : Generator rotor field winding current (measured data)

V_q : Q-axis component of generator terminal voltage (calculated from measurement, Vt, P, Q, etc.)

R_a : Stator winding resistance (from OEM)

L_l : Stator winding leakage inductance (from OEM)

S_a : A factor representing the degree of magnetic saturation at a given operating point, calculated based on OCC, between the air-gap flux and the stator-rotor combined magneto-motive-force.

Linear regression is used to eliminate the random measurement error which may exist in the field data. It is suggested to use not less than 15 points of online measurement data including terminal voltage V_t , active power P, reactive power Q, and field current I_{fd} , for using this method to calculate K_w .

A pair of characteristic saturation factors, i.e., S1.0 & S1.2, used to represent the generator open-circuit saturation characteristics, is needed. The saturation function type needs to be specified by setting the Sat_{Flag} in the GENQEC model parameter. Due to the sensitivity of the rotor angle measurement to the mechanical reference signal on the rotor shaft (especially for salient-pole machines), it is recommended to use generator's q-axis synchronous inductance, L_q , to calculate generator internal rotor angle when using this method. (The generator q-axis synchronous inductance can be validated using measurement



results with larger rotor angles where the measured values are less-susceptible to the mechanical reference.) Generator stator winding leakage inductance L_l (and resistance R_a , if known), are also needed in the calculation.

The unsaturated L_d in equation (1) is a constant per its definition, so the linear function at the left-hand side of equation (1) with reference to i_d should be reflected in the values calculated for all the measurement points on the right-hand of equation (1). In other words, the calculated values of the right-hand side of equation (1) shall conform to a distribution along a linear line in a plot with i_d on X-axis. The only undetermined variable K_w in equation (1) can be chosen in equation (1) such that we can use linear regression with all the online measurement points on the right-hand side of equation (1) to form a most-suitable linear line.

More detailed explanation about this method is illustrated with example steps below.

Step 1. Gather parameters and field measurements for calculation

First step is to gathering generator information needed for calculating K_w . That includes the data from manufacture and field measurement. Those data are listed as an example in table 2 and 3 below.

Table 2. 83.5 MVA Salient-pole Generator Parameters

| Sbase(MVA) | Vt _{base} (kV) | L_l | L_q | $S_{1.0}$ | $S_{1.2}$ | R_a |
|------------|-------------------------|-------|-------|-----------|-----------|-------|
| 83.5 | 13.8 | 0.15 | 0.7 | 0.19 | 0.55 | 0.004 |

Table 3. 83.5 MVA Salient-pole Online Measurement Data

| No. | Active Power (MW) | Reactive Power (Mvar) | Terminal Voltage (kV) | Field Current (A) | No. | Active Power (MW) | Reactive Power (Mvar) | Terminal Voltage (kV) | Field Current (A) |
|-----|-------------------|-----------------------|-----------------------|-------------------|-----|-------------------|-----------------------|-----------------------|-------------------|
| 1 | -0.44 | -38.62 | 13.26 | 255 | 34 | 40.02 | -19.49 | 13.55 | 495 |
| 2 | -0.45 | -32.44 | 13.40 | 305 | 35 | 40.48 | -15.29 | 13.59 | 529 |
| 3 | -0.57 | -29.61 | 13.47 | 330 | 36 | 40.11 | -10.74 | 13.63 | 560 |
| 4 | -0.49 | -25.25 | 13.50 | 361 | 37 | 40.11 | -4.92 | 13.67 | 604 |
| 5 | -0.61 | -20.91 | 13.54 | 395 | 38 | 40.21 | -0.53 | 13.7 | 650 |
| 6 | -0.73 | -13.58 | 13.50 | 442 | 39 | 40.09 | 5.52 | 13.76 | 699 |
| 7 | -0.75 | -12.12 | 13.61 | 465 | 40 | 40.23 | 9.98 | 13.78 | 744 |
| 8 | -0.78 | -4.75 | 13.67 | 526 | 41 | 40.29 | 14.4 | 13.82 | 784 |
| 9 | -0.67 | -0.2 | 13.71 | 565 | 42 | 40.08 | 20.49 | 13.87 | 844 |
| 10 | -0.82 | 5.75 | 13.75 | 621 | 43 | 40.1 | 26.58 | 13.92 | 908 |
| 11 | -0.91 | 10.22 | 13.79 | 664 | 44 | 40.29 | 31.27 | 13.95 | 961 |
| 12 | -1 | 14.7 | 13.83 | 712 | 45 | 40.24 | 42.19 | 14.04 | 1090 |

| | | | | | | | | | |
|----|-------|--------|-------|------|----|-------|--------|-------|------|
| 13 | -0.96 | 19.26 | 13.86 | 758 | 45 | 59.74 | -20.71 | 13.53 | 585 |
| 14 | -1.07 | 25.11 | 13.94 | 825 | 47 | 59.55 | -14.4 | 13.58 | 625 |
| 15 | -0.83 | 29.89 | 14.03 | 887 | 48 | 60.04 | -9.97 | 13.63 | 655 |
| 16 | -0.89 | 33.89 | 14.10 | 938 | 49 | 60.22 | -5.44 | 13.65 | 689 |
| 17 | 20.38 | -36.5 | 13.40 | 315 | 50 | 59.67 | 0.4 | 13.71 | 740 |
| 18 | 20.67 | -28.73 | 13.47 | 365 | 51 | 59.83 | 4.82 | 13.75 | 777 |
| 19 | 20.82 | -24.36 | 13.51 | 399 | 52 | 59.21 | 9.4 | 13.79 | 818 |
| 20 | 20.71 | -21.52 | 13.53 | 419 | 53 | 59.7 | 15.28 | 13.82 | 874 |
| 21 | 20.64 | -15.82 | 13.58 | 464 | 54 | 60.1 | 21.36 | 13.87 | 933 |
| 22 | 20.67 | -9.87 | 13.63 | 511 | 55 | 60.05 | 24.38 | 13.89 | 962 |
| 23 | 20.54 | -5.59 | 13.67 | 543 | 56 | 59.71 | 31.57 | 13.96 | 1036 |
| 24 | 20.39 | 1.11 | 13.72 | 600 | 57 | 60.05 | 33.55 | 13.97 | 1060 |
| 25 | 20.35 | 5.55 | 13.75 | 644 | 58 | 80.13 | -9.12 | 13.62 | 774 |
| 26 | 20.3 | 10.04 | 13.79 | 688 | 59 | 80.09 | -6.04 | 13.64 | 794 |
| 27 | 20.32 | 14.49 | 13.82 | 732 | 60 | 80.1 | -0.3 | 13.69 | 841 |
| 28 | 20.55 | 22.04 | 13.89 | 810 | 61 | 80.07 | 5.71 | 13.74 | 891 |
| 29 | 20.41 | 26.63 | 13.90 | 859 | 62 | 80.07 | 10.04 | 13.77 | 929 |
| 30 | 20.38 | 32.73 | 13.97 | 929 | 63 | 79.97 | 14.63 | 13.81 | 971 |
| 21 | 20.32 | 40.76 | 14.03 | 1029 | 64 | 80.02 | 20.63 | 13.86 | 1028 |
| 32 | 40.02 | -27.26 | 13.49 | 444 | 65 | 80.08 | 21.71 | 13.87 | 1037 |
| 33 | 40.05 | -25.33 | 13.50 | 459 | | | | | |

Step 2. Determine field current base value

Before the measured field current can be converted to per unit, a field current base value is needed. Typically, the field current base value is obtained from open-circuit saturation test results when the measured terminal voltage is plotted against the field current. In the absence of the good open-circuit test data, the field current base value can be determined as below:

Reorganizing equation (1), noting that $I_{fd} = I_{fd_meas}/I_{fd_base}$, where I_{fd_meas} is the measured field current in amperes and I_{fd_base} is the field current base in amperes, we have:

$$\frac{1-K_w i_d}{I_{fd_base}} = \frac{(1+S_a)(V_q+R_a i_q)+S_a L_l i_d+L_d i_d}{I_{fd_meas}} \quad (2)$$

The right-hand side of Equation (2) is calculated from measurement data for each operating point and plotted against i_d . The K_w on the left-hand side of (2) is also one factor to be determined in this expression, and it is independent from i_d in the right-hand expression. The most important observation from (2) is that I_{fd_base} can be determined with $i_d=0$ when the left-hand side of (2) becomes $1/I_{fd_base}$. Using polynomial trend plot based on the calculated values of the right-hand expression of (2) against i_d , let $i_d=0$, the field current base value obtained from the online measurements for this unit is 492.5A.



Step 3. Linear regression on L_d to determine K_w

Linear regression method is applied to the calculated values of the right-hand side of equation (1) with reference to i_d . Since K_w is also undetermined, the criterion used is to decide the most-straight line of ($L_d i_d$) by adjusting K_w .

Fig. 2 shows the calculated $y = L_d i_d$ as a function of i_d when K_w is set to zero, where linear and second-order polynomial trend lines are plotted. Fig. 3 shows the calculated $L_d i_d$ when K_w is set to a value of 0.4, also with linear and second-order polynomial trend lines plotted. It can be observed that the polynomial trendline curves upwards with $K_w=0$ but downwards with $K_w=0.4$. Based on the involvement of K_w in equation (1), it is reasonable to expect that between 0 and 0.4 there exists a K_w value which could make the polynomial trendline closely overlays with the linear one. By gradually adjusting K_w value, it is found that $K_w=0.2235$ gives the best match between the second-order polynomial and linear trendlines, as can be seen in Fig. 4. The two trend lines are virtually overlapping each other. The trendline equations in Fig. 4 also provide the ideal L_d value with the chosen K_w . Statistically with all the measurement points considered, this $L_d=0.982$ with $K_w=0.2235$ will have the best modeling results with least error.

Once this pair of L_d and K_w having the least linear regression error on L_d is found, the corresponding differences (or errors) of the modeled field current for each measurement points are also known from the calculation.

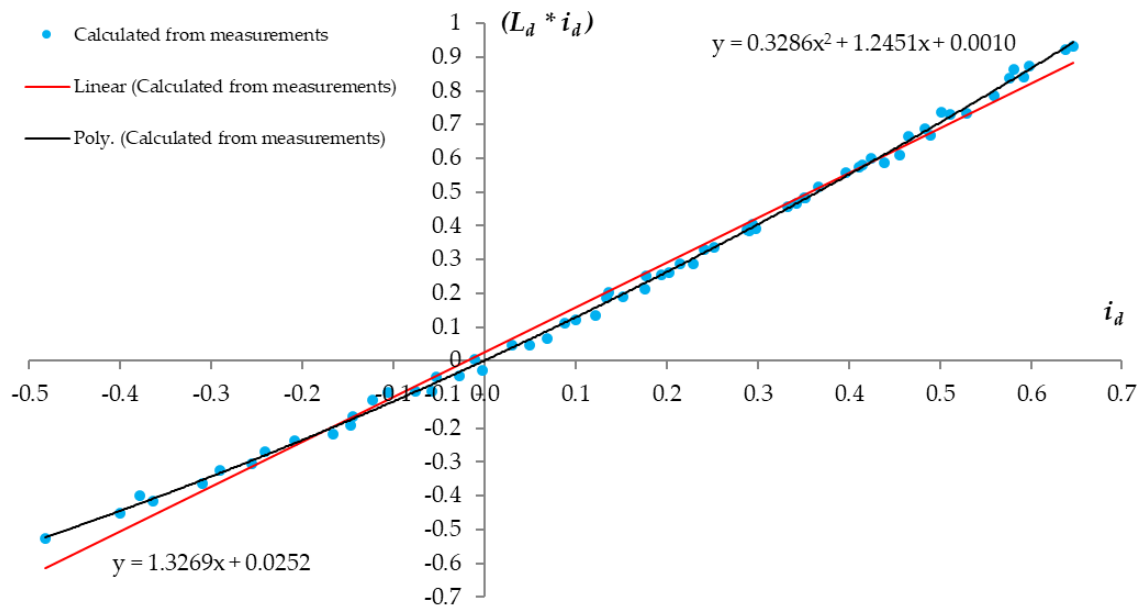


Fig. 2. Online measurements calculated $L_d i_d$ with $K_w = 0$

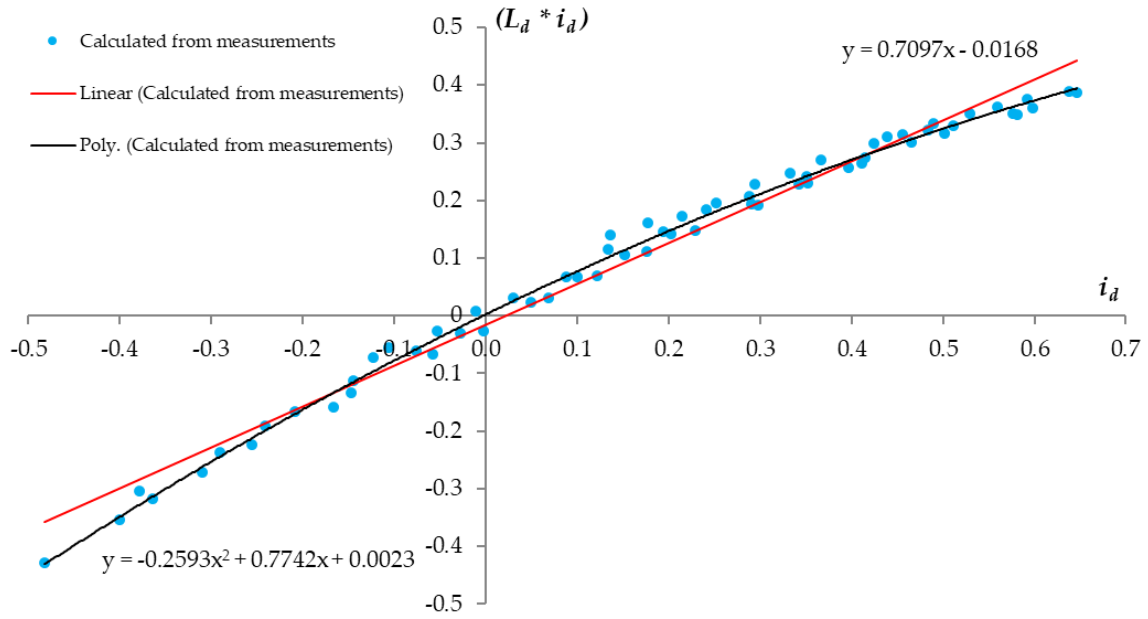


Fig. 3. Online measurements calculated $L_d i_d$ with $K_w = 0.4$

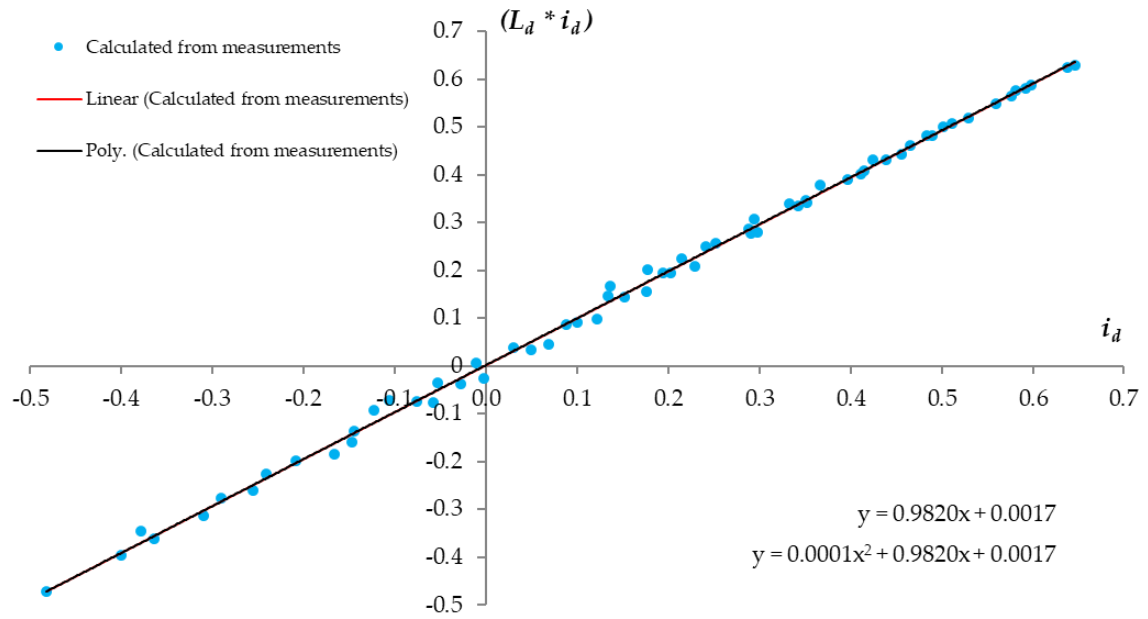


Fig. 4. Online measurements calculated $L_d i_d$ with $K_w = 0.2235$

Step 4. (Optional) VEE Curve Results Comparison with Determined L_d and K_w

Previous three steps illustrated a whole process of obtaining K_w , as well as L_d . The step 4 using VEE curve can be used as an option to double check the K_w value. The Fig 5 and Fig 6 below are the VEE curve plots using K_w achieved from step 3 for the same generator in the example.

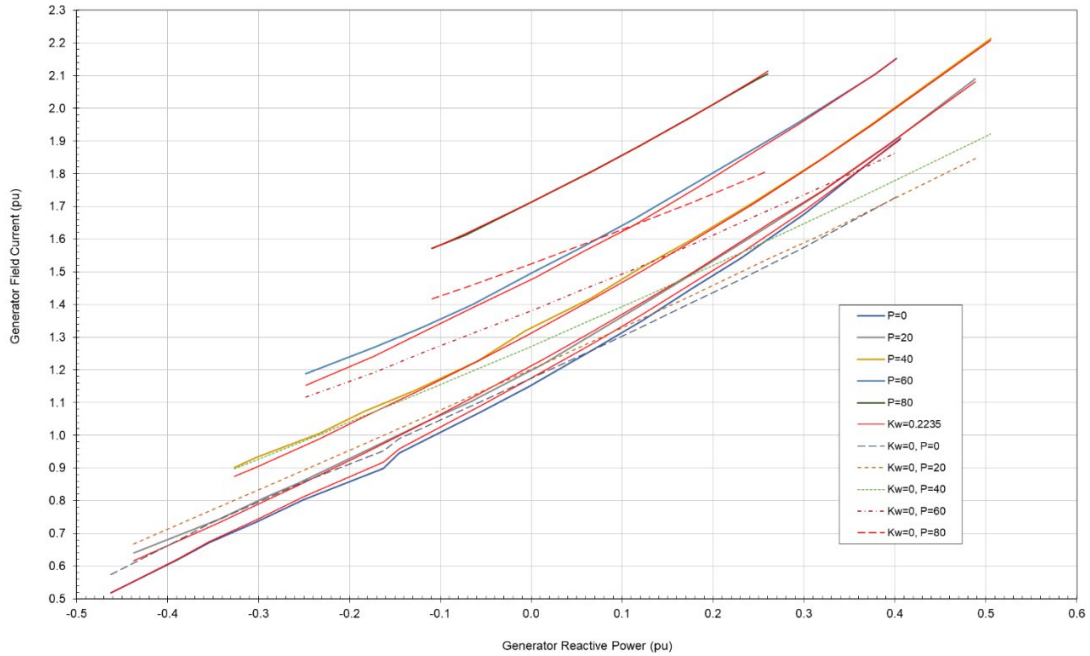


Fig. 5. Measured and modeled field current comparison with reference to reactive power

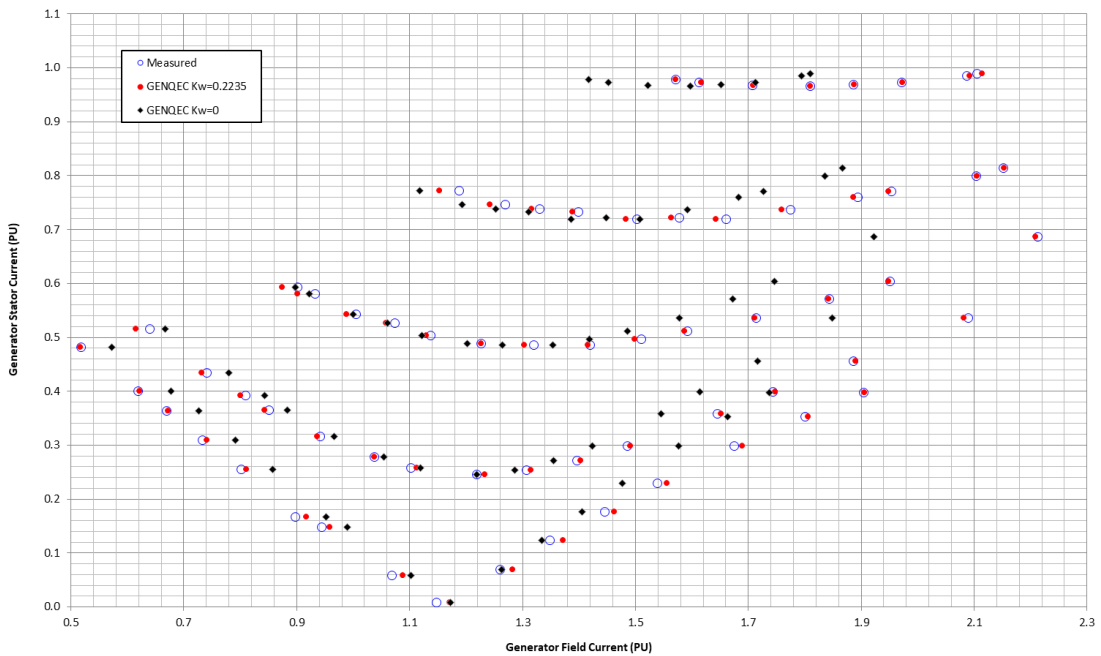


Fig. 6. Measured and modeled field current comparison with reference to stator current

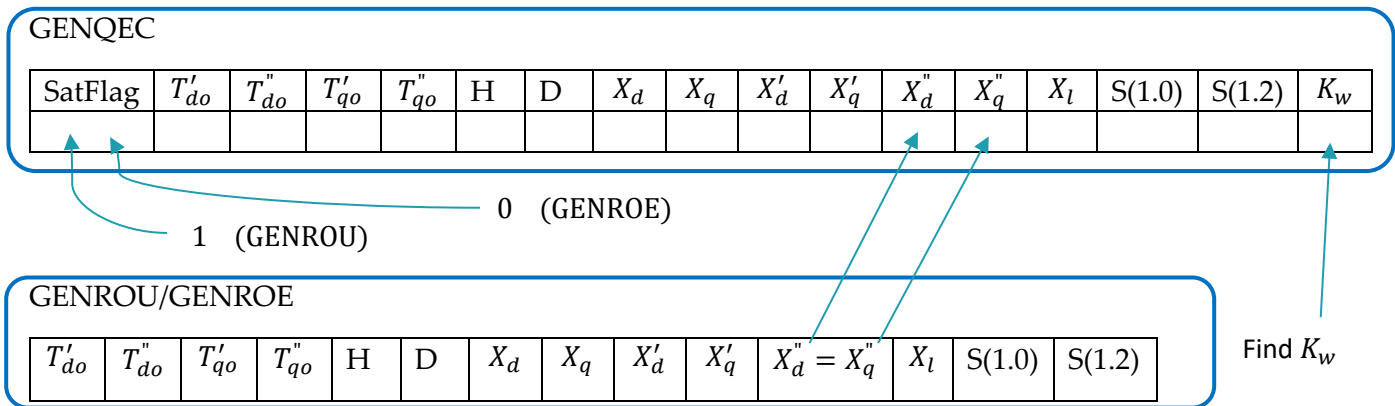


Existing generator model migration to GENQEC

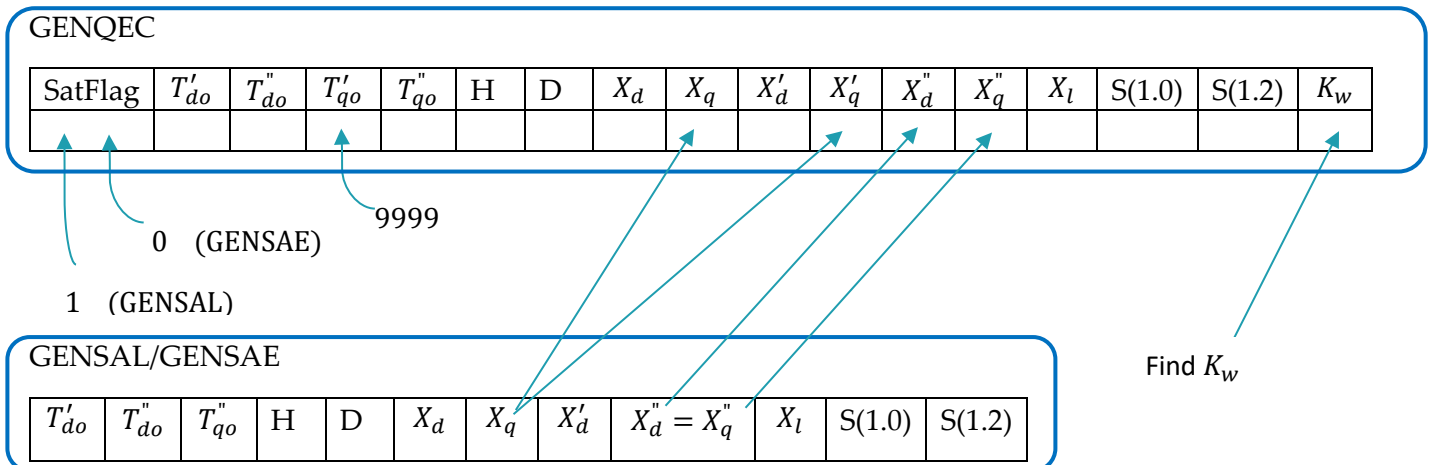
Generator models based on the second-order equivalent circuits can be simply converted to GENQEC once the K_w is determined. These second-order equivalent-circuit based models include GENROU, GENROE, GENSAL and GENSAE. It is not recommended to perform direct parameter mapping from GENTPJ to GENQEC, because of the possible modification of GENTPJ to the model parameters when converted from the earlier models.

In the parameter conversion, the parameters in GENQEC are mapped one-to-one directly from the earlier second-order generator models, except those parameters explicitly marked below.

Round-rotor generator (GENROU, GENROE to GENQEC)



Salient-pole generator (GENSAL, GENSAE to GENQEC)



(For GE PSLF™ program, the quadratic saturation model in GENROU and GENSAL may need to use SatFlag = 2 when converting to GENQEC. Using SatFlag=2 will still keep the same compatibility level between the Siemens/PTI PSS®E and GE PSLF using the previous models.)



Appendix A

GENQEC model block diagram and its equivalent circuit representation

Nomenclature

- i_d : D-axis component of generator stator current
 i_q : Q-axis component of generator stator current
 V_q : Q-axis component of generator stator voltage
 I_{fd} : Generator rotor field winding current
 E_{fd} : Generator rotor field winding voltage
 R_a : Generator stator winding resistance
 L_d : Generator direct-axis synchronous inductance, ($L_d = L_{ad} + L_l$)
 L_q : Generator quadrature-axis synchronous inductance
 S_a : A factor representing the degree of magnetic saturation at a given operating point, reflected in the generator's open-circuit saturation characteristics
 K_w : A factor in the GENQEC model to compensate I_{fd} for the field winding leakage variation associated with i_d
 L_l : Stator winding leakage inductance
 L_{ad} : Stator to rotor winding d-axis mutual inductance
 L_{fd} : Rotor field winding leakage inductance
 L_{1d} : Rotor d-axis damper winding leakage inductance
 R_{1d} : Rotor d-axis damper winding resistance
 R_{fd} : Rotor field winding resistance
 ψ_d : Stator winding d-axis total flux
 ψ_{1d} : Rotor d-axis damper winding total flux
 ψ_{fd} : Rotor field winding total flux
 $L_{11d} = L_{ad} + L_{1d}$: Rotor d-axis damper winding inductance
 $L_{ffd} = L_{ad} + L_{fd}$: Rotor field winding self-inductance

GENQEC D-axis Saturation

GENQEC model considers the magnetic saturation primarily on the mutual inductance between the generator rotor and stator windings, as shown in Fig. A-1. The inclusion of magnetic saturation on rotor windings'

leakages is for the benefit of using the classical representation of the generator "standard" parameters, as can be seen from the derivation process given below.

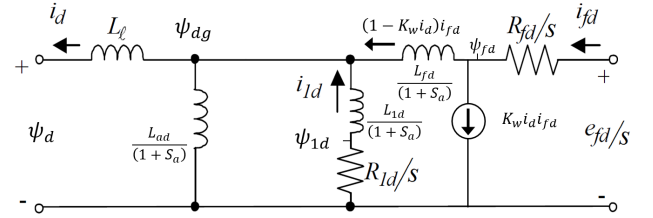


Fig. A-1 GENQEC D-axis equivalent circuit

From Fig. A-1 equivalent circuit represented using the L_{ad} -base reciprocal per unit system, we can obtain below equations:

$$\psi_d = \frac{-L_{ad}i_d - S_d L_l i_d}{(1+S_d)} + \frac{L_{ad}(1-K_w i_d)i_{fd}}{(1+S_d)} + \frac{L_{ad}i_{1d}}{(1+S_d)} \quad (\text{A-1})$$

$$\psi_{fd} = \frac{-L_{ad}i_d}{(1+S_d)} + \frac{L_{ffd}(1-K_w i_d)i_{fd}}{(1+S_d)} + \frac{L_{ad}i_{1d}}{(1+S_d)} \quad (\text{A-2})$$

$$\psi_{1d} = \frac{-L_{ad}i_d}{(1+S_d)} + \frac{L_{ad}(1-K_w i_d)i_{fd}}{(1+S_d)} + \frac{L_{11d}i_{1d}}{(1+S_d)} \quad (\text{A-3})$$

$$e_{fd} = s\psi_{fd} + R_{fd}i_{fd} \quad (\text{A-4})$$

$$0 = s\psi_{1d} + R_{1d}i_{1d} \quad (\text{A-5})$$

To convert to the commonly used per unit system in power system stability studies, we use base values denoted with an overbar accent, which have below relations with the L_{ad} -base reciprocal per unit system:

$$\overline{\psi_d} = \psi_d \quad (\text{A-6})$$

$$\overline{i_d} = i_d \quad (\text{A-7})$$

$$\overline{\psi_{1d}} = \psi_{1d} \quad (\text{A-8})$$

$$\overline{i_{1d}} = i_{1d} \quad (\text{A-9})$$

$$\overline{I_{fd}} = L_{ad}i_{fd} \quad (\text{A-10})$$

$$\overline{\psi}_{fd} = \frac{L_{ad}}{L_{ffd}} \psi_{fd} \quad (\text{A-11})$$

$$\overline{E}_{fd} = \frac{L_{ad}}{R_{fd}} e_{fd} \quad (\text{A-12})$$

Using (A-6), (A-7), (A-9) and (A-10), Eq. (A-1) can be re-written as:

$$(1 + S_d)\overline{\psi}_{fd} = -L_d\overline{i}_{fd} - S_d L_l \overline{i}_{fd} + (1 - K_w i_d)\overline{I}_{fd} + \frac{L_{ad}}{L_{ad}} \overline{i}_{1d} \quad (\text{A-13})$$

Apply (A-7), (A-9), (A-10) and (A-11) to (A-2), we have:

$$(1 + S_d)\overline{\psi}_{fd} = -\frac{L_{ad}^2}{L_{ffd}} \overline{i}_{fd} + (1 - K_w i_d)\overline{I}_{fd} + \frac{L_{ad}^2}{L_{ffd}} \overline{i}_{1d} \quad (\text{A-14})$$

In generator's second-order model, the classical representation of d-axis transient inductance L'_d (a standard parameter) is defined as: L_{ad} in parallel with L_{fd} , then added to the stator leakage L_l ; i.e., $L'_d = \frac{L_{ad}L_{fd}}{L_{ad}+L_{fd}} + L_l$. Consider the definition of L_d and L_{ffd} , below relation exists:

$$L_d - L'_d = \frac{L_{ad}^2}{L_{ffd}} \quad (\text{A-15})$$

Eq. (A-14) can be re-written as:

$$(1 + S_d)\overline{\psi}_{fd} = (1 - K_w i_d)\overline{I}_{fd} + (L_d - L'_d)(\overline{i}_{1d} - \overline{i}_{fd}) \quad (\text{A-16})$$

Using (A-7) to (A-10), Eq. (A-3) can be re-written as:

$$(1 + S_d)\overline{\psi}_{1d} = -L_{ad}\overline{i}_{1d} + (1 - K_w i_d)\overline{I}_{fd} + L_{11d}\overline{i}_{1d} \quad (\text{A-17})$$

Apply (A-10), (A-11) and (A-12) to Eq. (A-4),

$$\frac{R_{fd}}{L_{ad}} \overline{E}_{fd} = s \frac{L_{ffd}}{L_{ad}} \overline{\psi}_{fd} + \frac{R_{fd}}{L_{ad}} \overline{I}_{fd} \quad (\text{A-18})$$

After simplification,

$$\overline{E}_{fd} = s \frac{L_{ffd}}{R_{fd}} \overline{\psi}_{fd} + \overline{I}_{fd} \quad (\text{A-19})$$

Generator's d-axis open-circuit transient time constant is defined as $T'_{do} = \frac{L_{ffd}}{R_{fd}}$ according to its classical representation. We have:

$$\overline{E}_{fd} = sT'_{do} \overline{\psi}_{fd} + \overline{I}_{fd} \quad (\text{A-20})$$

Eq. (A-5) can be re-written using Eqs. (A-8) and (A-9),

$$0 = s \overline{\psi}_{1d} + R_{1d} \overline{i}_{1d} \quad (\text{A-21})$$

The relations given in Eqs. (A-13), (A-16), (A-17), (A-20) and (A-21) can be expressed using the classical representation of the standard generator model parameters, with mathematical derivations shown below.

Subtract Eq. (A-17) from Eq. (A-16), we have:

$$(1 + S_d)(\overline{\psi}_{fd} - \overline{\psi}_{1d}) = (L'_d - L_l)\overline{i}_{fd} - (L'_d - L_l + L_{1d})\overline{i}_{1d} \quad (\text{A-22})$$

From Eq. (A-21), $\overline{i}_{1d} = -\frac{s \overline{\psi}_{1d}}{R_{1d}}$. Define the generator d-axis open-circuit sub-transient time constant $T''_{do} = \frac{L'_d - L_l + L_{1d}}{R_{1d}}$, the above equation becomes:

$$(1 + S_d)(\overline{\psi}_{fd} - \overline{\psi}_{1d}) = (L'_d - L_l)\overline{i}_{fd} + sT''_{do} \overline{\psi}_{1d} \quad (\text{A-23})$$

When the generator d-axis sub-transient inductance L''_d is defined using its classical representation, $L''_d = \frac{L_{ad}L_{fd}L_{1d}}{L_{ad}L_{fd}+L_{1d}L_{fd}+L_{1d}L_{ad}} + L_l$. It can be proven that $\frac{1}{L'_d - L_l + L_{1d}} = \frac{L'_d - L''_d}{(L'_d - L_l)^2}$.

Accordingly, from Eq. (A-21),

$$\overline{i}_{1d} = -\frac{sT''_{do} \overline{\psi}_{1d}}{L'_d - L_l + L_{1d}} = -\frac{L'_d - L''_d}{(L'_d - L_l)^2} sT''_{do} \overline{\psi}_{1d} \quad (\text{A-24})$$

Note that the above parameters of T'_{do} , T''_{do} , L'_d and L''_d are all defined according to the classical representation of the standard parameters of second-order generator model described in Chapter 4 of Prabha Kundur's *Power System Stability and Control* [7].

From Fig. A-1, the L_{ad} -base reciprocal per unit system representation, we can see,

$$\frac{(\psi_{1d} - \psi_{dg})(1 + S_d)}{L_{1d}} + \frac{(\psi_{fd} - \psi_{dg})(1 + S_d)}{L_{fd}} = i_d + \frac{\psi_{dg}(1 + S_d)}{L_{ad}} \quad (\text{A-25})$$



It can also be written as

$$\frac{\psi_{1d}}{L_{1d}} + \frac{\psi_{fd}}{L_{fd}} = \frac{i_d}{1+S_d} + \psi_{dg} \left(\frac{1}{L_{ad}} + \frac{1}{L_{fd}} + \frac{1}{L_{1d}} \right) = \frac{i_d}{1+S_d} + \psi_{dg} \left(\frac{1}{L'_d - L_l} \right) \quad (A-26)$$

Also from Fig. A-1, $\psi_{dg} = \psi_d + L_l i_d$. Substitute ψ_{dg} into (A-26),

$$\frac{(L''_d - L_l)\psi_{1d}}{L_{1d}} + \frac{(L''_d - L_l)\psi_{fd}}{L_{fd}} = \psi_d + L_l i_d + \frac{(L''_d - L_l)i_d}{1+S_d} \quad (A-27)$$

The relation below can be easily obtained:

$$\frac{L''_d - L_l}{L_{1d}} = \frac{L_{ad}L_{fd}}{L_{ad}L_{fd} + L_{ad}L_{1d} + L_{1d}L_{fd}} = \frac{L'_d - L''_d}{L'_d - L_l} \quad (A-28)$$

In addition, the second term on the left-hand side of Eq. (A-27) can be changed to commonly-used per-unit system:

$$\frac{L''_d - L_l}{L_{fd}} \psi_{fd} = \frac{L''_d - L_l}{L_{fd}} \overline{\psi_{fd}} \frac{L_{ffd}}{L_{ad}} = \frac{L''_d - L_l}{L'_d - L_l} \overline{\psi_{fd}} \quad (A-29)$$

Substitute Eqs. (A-28) and (A-29) into Eq. (A-27), also noting $\overline{\psi_d} = \psi_d$ and $\overline{i_d} = i_d$,

$$\frac{L'_d - L''_d}{L'_d - L_l} \overline{\psi_{1d}} + \frac{L''_d - L_l}{L'_d - L_l} \overline{\psi_{fd}} = \overline{\psi_d} + L_l \overline{i_d} + \frac{(L''_d - L_l)}{1+S_d} \overline{i_d} \quad (A-30)$$

We can use Eqs. (A-16), (A-20), (A-23), (A-24) and (A-30) to construct a block diagram, shown in the top half of Fig. A-2, the complete GENQEC model block diagram. The overbar notation is dropped, considering only the commonly used per unit system exists in stability analysis. GRNQEC model structure is similar to the previous GENROU/GENSAE model except the implementation of the magnetic saturation and field current compensation factor K_w .

GENQEC Q-axis Saturation

From Fig. A-3 GENQEC q-axis equivalent circuit, following the same derivation process (omitted here), we can obtain the lower half of the block diagram shown in Fig. A-2.

GENQEC dynamic model can be completely represented either using its equivalent circuits in Figs. A-1 and A-3, or using the block diagram in Fig. A-2 (with network interfaces added.)

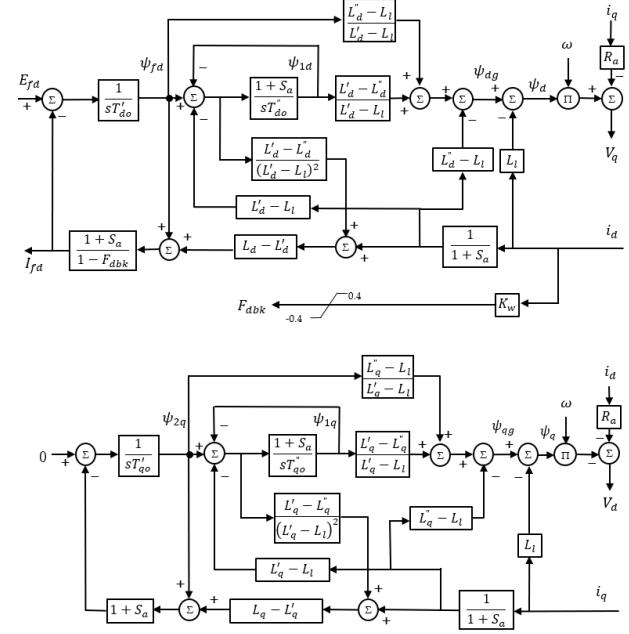


Figure A-2: GENQEC Model Block Diagram

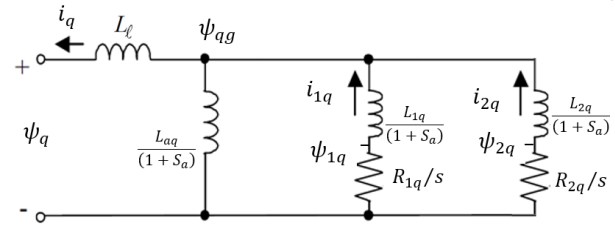


Fig. A-3 GENQEC Q-axis equivalent circuit

References:

- [1] Mohamed Elkhatib, Xiaokang Xu, Song Wang and Quincy Y. Wang, "Implementation and Benchmarking of a New Generator Dynamic Model for Power System Stability Analysis," presented and in Proc. of the IEEE PES General Meeting, 25-29 July 2021, Washington, DC.
- [2] Quincy Wang, Song Wang, "Practical Improvements to Generator Parameter Validation using Stator-Decrement Test", IEEE Transactions on Energy Conversion, Digital Object Identifier: 10.1109/TEC.2021.3094822



- [3] Quincy Wang (2020, September). GENQEC Generator Dynamic Model Specification. [Online]. <https://www.wecc.org/>
- [4] Quincy Wang, Renke Huang, Song Wang, Ruisheng Diao, Yilu Liu, “Dynamic Performance of a High Accuracy Generator Dynamic Model for Stability Analysis”, 2019 IEEE PES Innovative Smart Grid Technology (ISGT) Asia, May 21-24, 2019, Chengdu, P. R. China
- [5] Quincy Wang, Song Wang, “A New High Accuracy Generator Dynamic Model”, IEEE PES Asia-Pacific Power and Energy Engineering Conference (APPEEC) 2018, October 7-10, 2018, Kota Kinabalu, Sabah, Malaysia
- [6] James Weber, “Comparison of Mathematic Models of GENQEC and GENOPZ”, MVS April 2021 meeting. [Online]. <https://www.wecc.org/>
- [7] P. Kundur, Power System Stability and Control, New York: McGraw-Hill, 1994.